Research Journal of Applied Sciences, Engineering and Technology 7(11): 2336-2344, 2014
DOI:10.19026/rjaset.7.534
ISSN: 2040-7459; e-ISSN: 2040-7467

Submitted: August 01, 2013 Accepted: August 12, 2013 Published: March 20, 2014

Research Article

Circuit Modeling of Ultra Wideband (UWB) Microstrip Patch Antenna Bending Effect

Lee Chia Ping and Chandan Kumar Chakrabarty
Department of Electronics and Communication Engineering, Centre for RF and Microwave Engineering, UNITEN Putrajaya Campus, Km 7, Jalan IKRAM-UNITEN, 43009 Kajang, Selangor DarulEhsan, Malaysia

Abstract: This study describes the bending effect on an Ultra Wideband (UWB) microstrip patch antenna on the antenna performance in terms of impedance bandwidth and radiation pattern. Comparison is done between the UWB planar antenna and the bent UWB antenna. The bending effect causes shift in resonant frequencies with slight change in the impedance bandwidth. A circuit model comprising lumped elements is also developed to represent the antenna design to analyze the variation of the input matching of the antenna during bending. The finding shows that the UWB antenna bending is suitable for UWB application even though slight degradation is observed compared to the planar UWB antenna. The simulated results are discussed in detail for the planar UWB antenna and the bending effect on the antenna performance as according to UWB characteristics.

Keywords: Impedance bandwidth, lumped element circuit, planar antenna, radiation pattern, resonant frequency, return loss, S_{11}

INTRODUCTION

Ultra Wide Band (UWB) antennas have sparked great interest among researchers since the approval by Federal Communications Commission (FCC) in February 2002 for the allocation of UWB frequency spectrum from 3.1 to 10.6 GHz (FCC (Federal Communications Commission), 2002). UWB antennas are on demand for various applications such as medical imaging, wireless communication and radar tracking due to the UWB technology that enables high speed data rate and low power consumption. In recent years, the development of non-planar antennas is gaining interest due to the flexibility of being fitted on non-planar surfaces like modern aircrafts, armored vehicles or even for body centric applications (Amaro *et al*., 2011). Thus, it is necessary to analyze the effect of the antenna bending on UWB performance.

Related researches on antenna bending were done mainly aimed for body worn purpose (Galehdar and Thiel, 2007; Bai and Langley, 2010; Amaro *et al*., 2011). These literatures incorporated textile materials for the antenna design such as Zelt, Pure Copper Polyester Tafetta Fabric (PCPTF) and EBG patches. The bending curvatures chosen were such that they approximate parts of human torso; adult's leg and arm and child's arm. All studies showed shift of resonant frequency on the impedance bandwidth. Meanwhile, Kornek *et al*. (2010) did research on bent patch antenna on Molded Interconnect Device (MID) substrate, in which coaxial 50 Ohm feed was used and the multiple bending degrees were tested 3.67 mm away from the feed. It was observed that resonant frequencies shifted to higher frequencies and 60° bending led to the worst performance. A compensation approach was done by modifying the antenna design to curb the bending effect. Bai and Langley (2009) presented a paper on wearable EBG antenna bending and crumpling covering 2.45 and 5.8 GHz wireless network. Combination of antenna with EBG improved the bending performance at lower band with the frequency shift of 100 MHz.

This study presents the circuit modeling of the effect of UWB antenna bending on the antenna performance. Planar UWB microstrip antenna is first designed before being bent on different radii to analyze the effects on UWB input matching and impedance bandwidth. Simulations are conducted using CST Microwave Studio software. Then, an equivalent circuit comprising lumped elements is developed for each bent antenna using AWR Design Environment to analyze the perturbation of each component value incurred during the bending. Overall, while shifting of resonant frequencies is observed, the impedance bandwidth of UWB characteristic is negligibly affected. The radiation patterns observed on E-plane and H-plane still display similar patterns though broader patterns are observed in certain angles.

Corresponding Author: Lee Chia Ping, Department of Electronics and Communication Engineering, Centre for RF and Microwave Engineering, UNITEN Putrajaya Campus, Km 7, Jalan IKRAM-UNITEN, 43009 Kajang, Selangor DarulEhsan, Malaysia

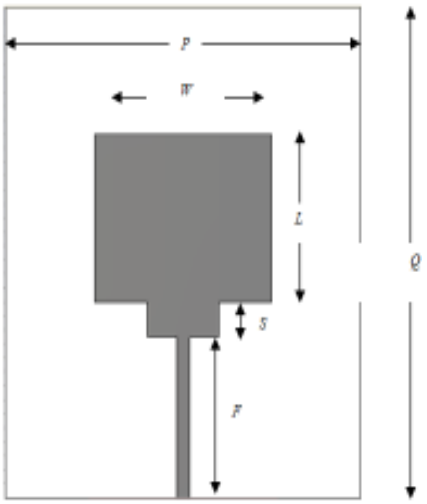

(a)

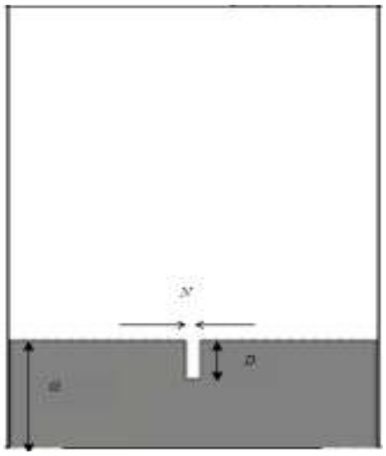

(b)

Fig. 1: Basic configuration of UWB microstrip patch antenna

METHODOLOGY

UWB microstrip patch antenna configuration: Figure 1 illustrates the basic configuration of UWB microstrip patch antenna. The proposed antenna comprises a radiator depicted as a larger rectangular patch truncated by a step, followed by a 50 Ohm microstrip feed line. The substrate used for the antenna designed is a Rogers RO4003 board with relative permittivity of 3.38. The radiator and feed line structure of antenna are designed on the front part of Rogers RO4003 substrate, backed by a partial ground plane with a notch on the other side of the substrate. The thickness of the substrate is 0.508 mm so as to suit the purpose of bending the antenna later. Simulations are done in optimizing the design parameters such as patch shape, feed line and ground plane before selecting the best dimensions to produce the best return loss, S_{11} and impedance bandwidth. The dimension of each design parameter is tabulated in Table 1.

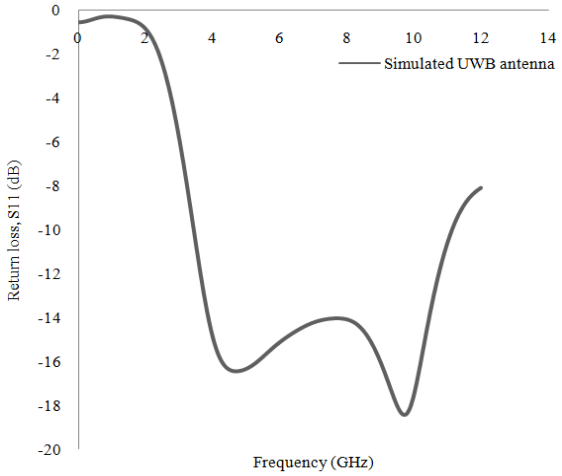

Fig. 2: Simulated return loss, S_{11} of the UWB microstrip patch antenna

Table 1: Dimension of UWB microstrip patch antenna

Variable	Dimension (mm)
P	30
Q	35
W	15
L	17
S	1.5
F	11.5
N	2.4
D	4
G	10

Figure 2 illustrates the simulated return loss, S_{11} of the UWB microstrip patch antenna. Without bending effect, the planar UWB antenna exhibits an impedance bandwidth from 3.43 to 11.12 GHz. The first resonant frequency observed at 4.78 GHz at -17.48 dB return loss is contributed by L of the patch length which is at resonant at TEM_{010} mode. The patch length is calculated to be at around 0.5λ using the equations as follow (Amaro *et al*., 2011):

$$L = \frac{\lambda}{2} \quad (1)$$

$$\lambda = \frac{c}{f_r\sqrt{\varepsilon_{ref}}} \quad (2)$$

where,
f_r = The resonant frequency
ε_{ref} = The effective permittivity

Meanwhile, the second resonant frequency observed at 9.78 GHz at return loss of -18 dB is contributed by the truncated step of the radiator patch, S. The existence of the second resonant frequency by truncated step is necessary to improve the impedance bandwidth of the antenna performance as it tunes the capacitive coupling between the radiator patch and the ground plane. The partial ground plane is designed with a notch in the middle to realize a series inductance. This particular structure has been investigated by Hoefer (1977) in which it is used to compensate for the excess

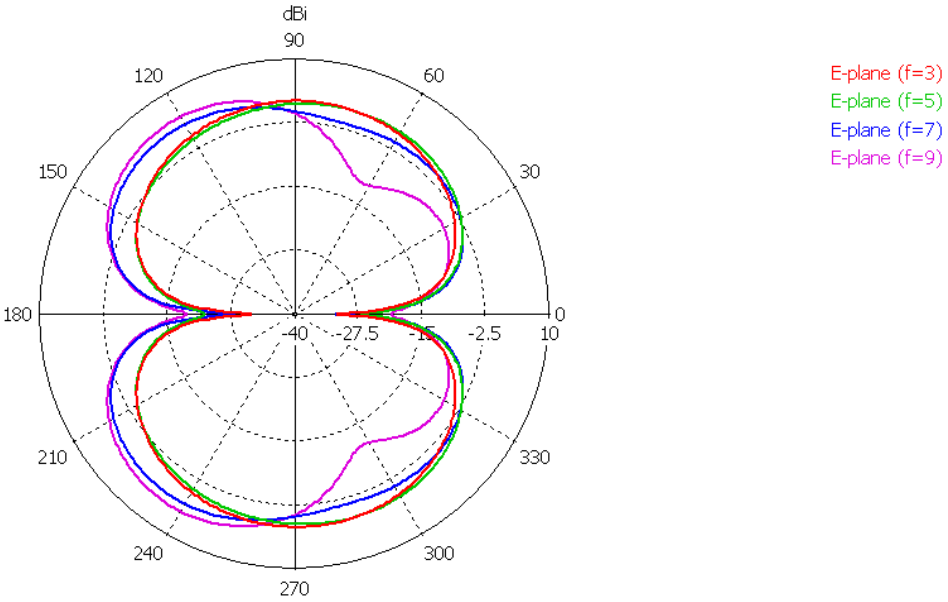

Fig. 3: Simulated radiation pattern of E-plane for planar UWB antenna

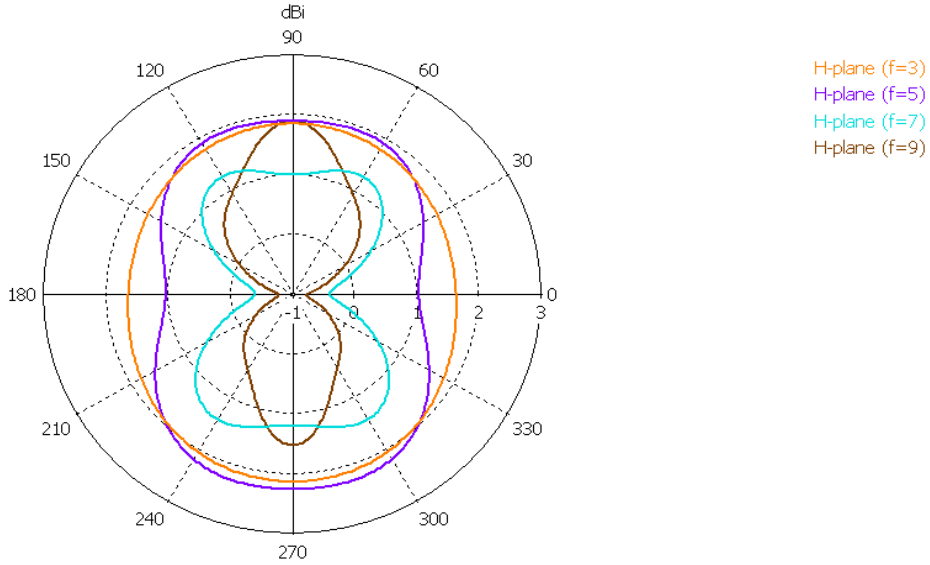

Fig. 4: Simulated radiation pattern of H-plane for planar UWB antenna

capacitance the discontinuities of the microstrip line, thereby maintaining a return loss, S_{11} graph of below -10 dB throughout the UWB impedance bandwidth.

Figure 3 illustrates the simulated radiation patterns of the E-plane at different frequencies from 3 to 9 GHz, at theta cut of 90°. It is observed that the radiation patterns at 3 and 5 GHz are similar to one another and display a directional behavior, with its main lobe direction at 90° and 270°. This indicates that the concentration of the field focuses on the front part and back part of the patch antenna respectively. Meanwhile, the lobes are suppressed at 0° and 180°, which originate from the sides of the patch. The radiation pattern at 7 GHz displays a slight difference where by the main lobe focuses at 135° and 225°. Nine-GHz radiation pattern also exhibits the main lobe direction in such way, but more lobes are observed from 90° to 270°. It is observed that the directivity of the antenna increases with increasing frequency, as the field gradually loses its concentration on the front and back part of the patch antenna as is observed from Fig. 3.

The radiation patterns of H-plane are also simulated at phi cut of 0° as shown in Fig. 4. The radiation pattern displays an omnidirectional pattern at 3 GHz while it is observed that there is a slight suppression at 0° and 180° at 5 GHz. More suppression

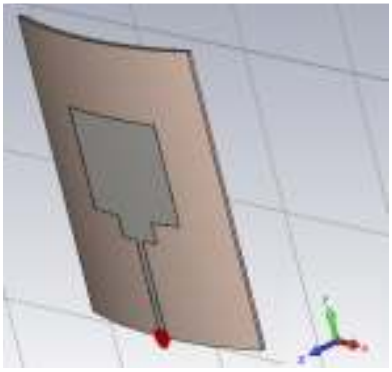

(a)

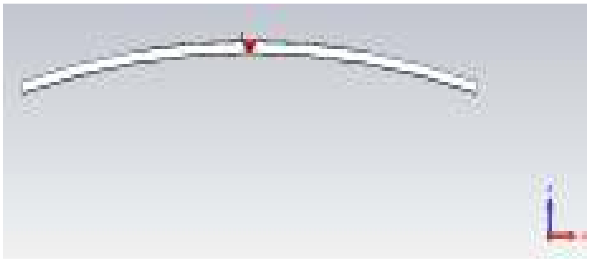

(b)

Fig. 5: Antenna bending along x-z plane

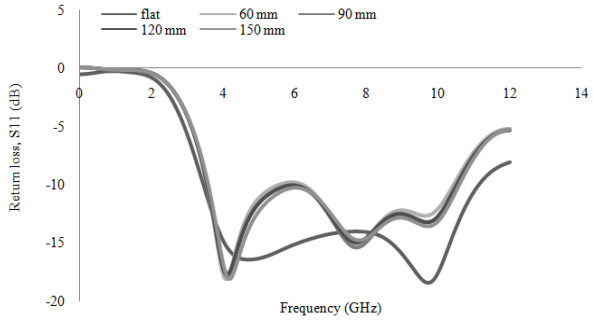

Fig. 6: Bending effect on impedance bandwidth using CST microwave studio

at the two angles is observed with increasing frequency at 7 and 9 GHz as the antenna directivity increases.

Bending effect on antenna performance: Using the same design and dimensions, the UWB microstrip patch antenna is bent over different cylindrical radii along the x-z principle plane with the antenna feed line placed along the cylindrical axis, as illustrated in Fig. 5. The antenna is bent over 150, 120, 90 and 60 mm, respectively cylinder and the bending effect on impedance bandwidth is displayed in Fig. 6. It is observed that the bending of the antenna does deteriorate the UWB antenna performance at the higher end frequency in terms of impedance bandwidth. Compared to the flat or planar antenna, the antenna bending also causes a shift in both resonant frequencies.

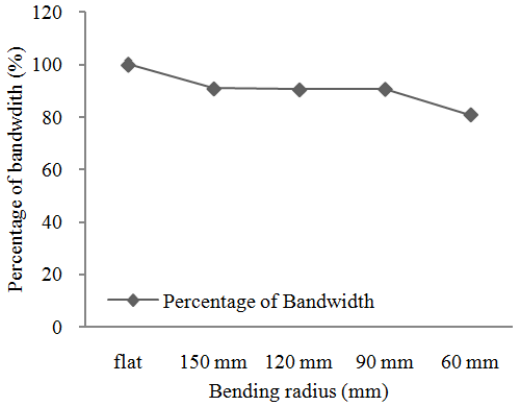

Fig. 7: Percentage of bandwidth achieved for all antenna bending radii

Table 2: Summary of resonant frequency shift during antenna bending

	Resonant frequency (GHz)		
Bending radius (mm)	f_1	f_2	f_3
Flat	4.78	9.78	-
150	4.16	9.80	7.79
120	4.11	9.74	7.71
90	4.12	9.74	7.70
60	4.07	9.74	7.69

More interestingly, the bending has caused an additional existence of resonant frequency around 7.7 GHz. While there is a distinctive difference at the higher end frequency of the impedance bandwidth between the unbent antenna and bent antenna, the antenna bending at all radii displays a similar pattern. Based on Fig. 6, when the antenna is more bent by decreasing the bending angle, it is observed that the first and third resonant frequencies are shifted up while the second frequency is shifted down. This indicates that the bending affects the resonant length of the antenna and thus causes the shift in the resonant frequencies, as validated by the study done by Salonen and Rahmat-Samii (2007). The reason for this frequency variation during the antenna bending was studied by Galehdar and Thiel (2007) as the change in mutual coupling between the radiating elements of the patch antenna. Table 2 summarizes the results of Fig. 6 in terms of the resonant frequency shift. It is also noted that the bending shifts the second resonant frequency to the extent that it pushes the graph to peak towards -10 dB in the region between 5.5 to 6.2 GHz. In fact, the antenna bending over the cylinder of 60 mm radius displays the graph peak at -9.78 dB, which does not fulfill the UWB bandwidth requirement of return loss less than -10 dB. Figure 7 illustrates the percentage of bandwidth achieved for all the antenna bending radii compared to the antenna without bending to visualize the severity of the degradation of the antenna performance.

Meanwhile, Fig. 8 illustrates the simulated radiation patterns of the E-plane at theta cut of 90° for

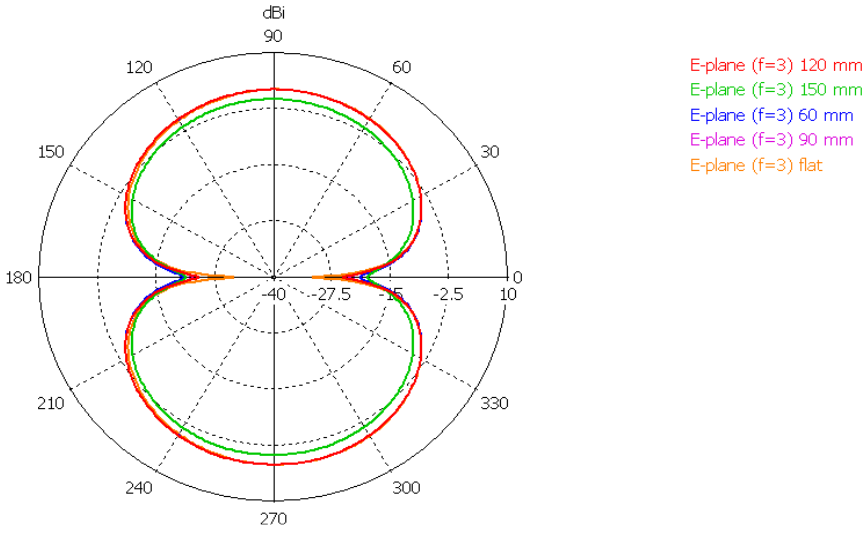
dBi
90
120
60
150
30
180
0
210
330
240
300
270
-40
-27.5
-15
-2.5
10
E-plane (f=3) 120 mm
E-plane (f=3) 150 mm
E-plane (f=3) 60 mm
E-plane (f=3) 90 mm
E-plane (f=3) flat

(a)

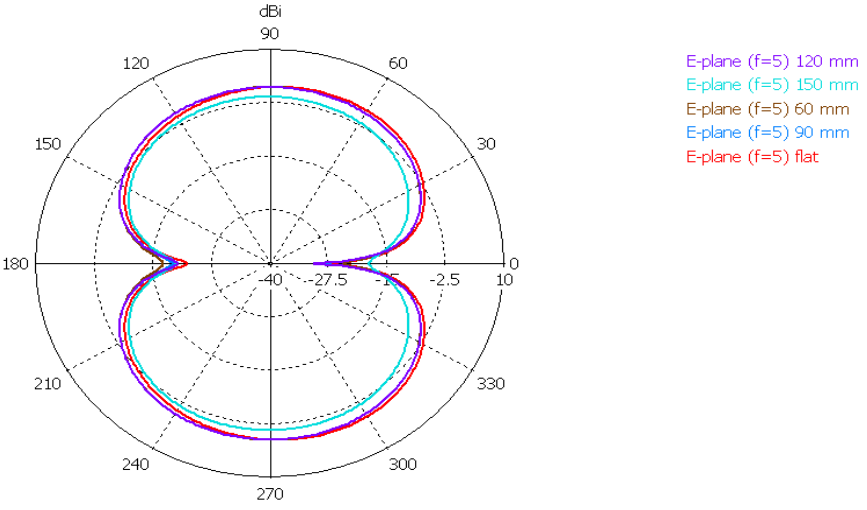
dBi
90
120
60
150
30
180
0
210
330
240
300
270
-40
-27.5
-15
-2.5
10
E-plane (f=5) 120 mm
E-plane (f=5) 150 mm
E-plane (f=5) 60 mm
E-plane (f=5) 90 mm
E-plane (f=5) flat

(b)

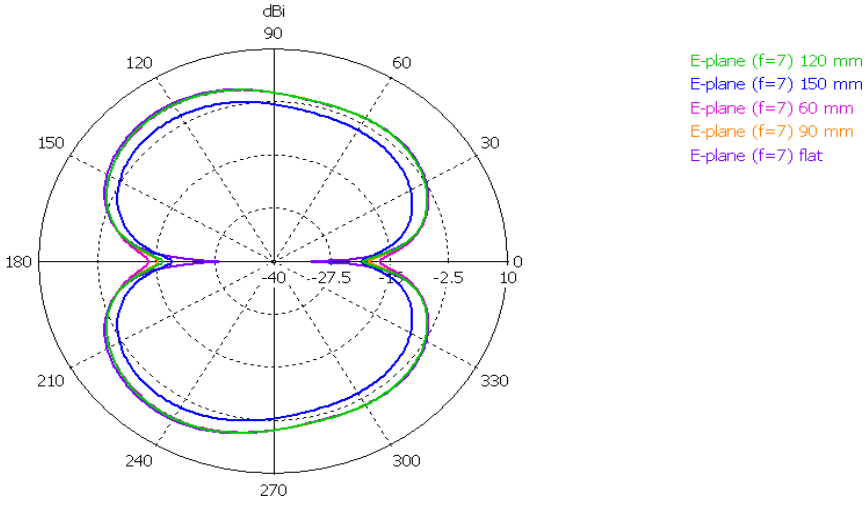
dBi
90
120
60
150
30
180
0
210
330
240
300
270
-40
-27.5
-15
-2.5
10
E-plane (f=7) 120 mm
E-plane (f=7) 150 mm
E-plane (f=7) 60 mm
E-plane (f=7) 90 mm
E-plane (f=7) flat

(c)

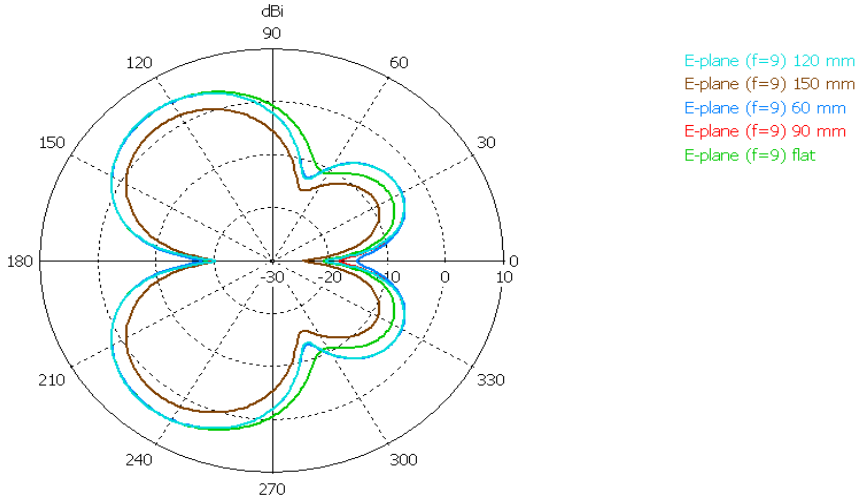

(d)

Fig. 8: Simulated radiation pattern of E-plane for all bending radii

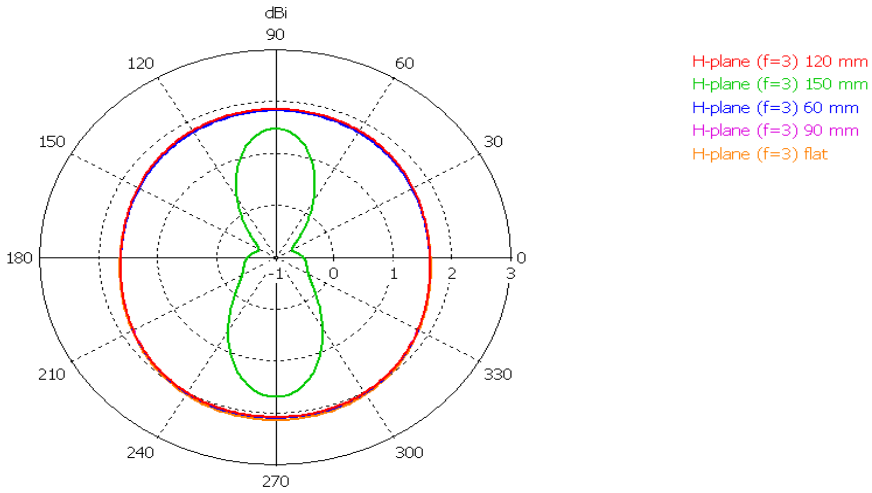

(a)

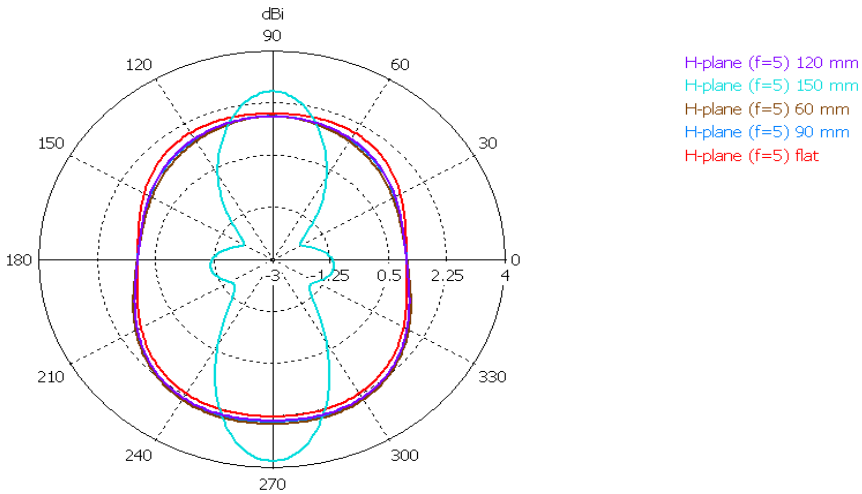

(b)

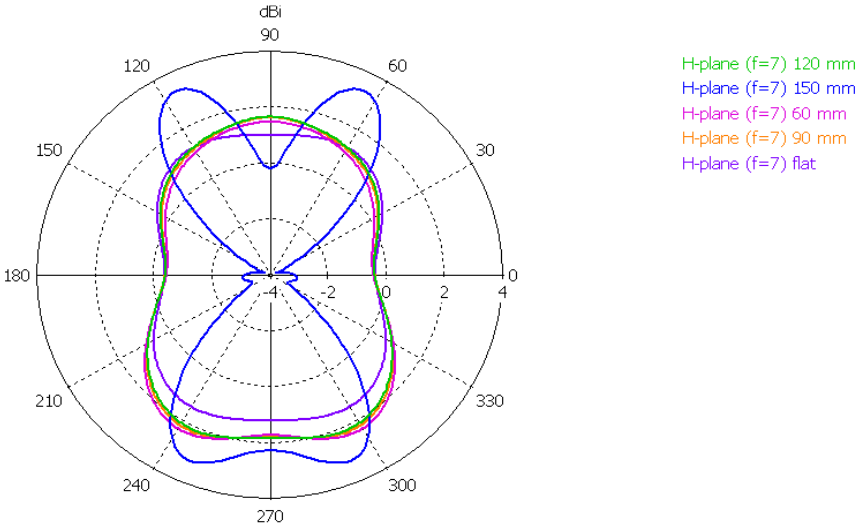

(c)

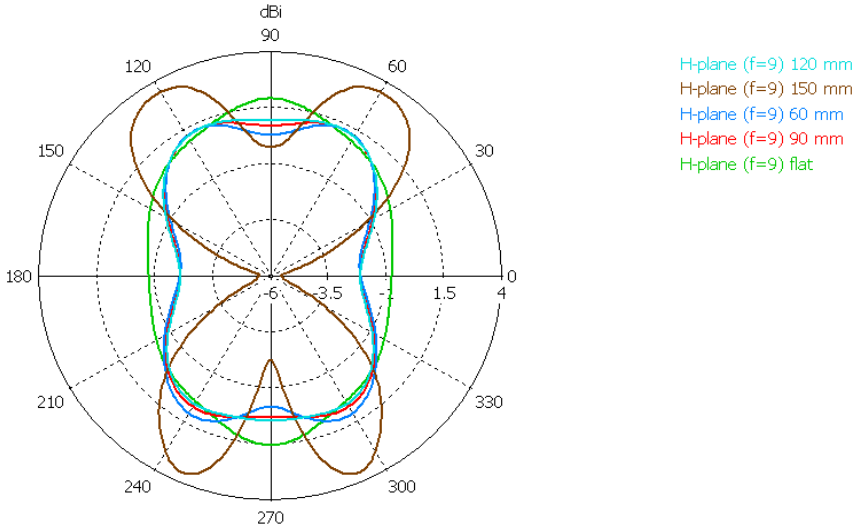

(d)

Fig. 9: Simulated radiation pattern of H-plane for all bending radii

all bending radii compared to the flat or planar UWB antenna. It is observed that the antenna bending still retains the radiation pattern shape for each frequency although it does broaden the radiation pattern mainly at 90° and 270°. Similar result was obtained in Kellomaki *et al*. (2006) for the bending of GPS antenna. The antenna directivity increases at the frequency of 9 GHz when the antenna is bent over 150 mm cylinder radius, but broadened radiation patterns are observed again as the bending angle increases.

Compared to the planar antenna, the radiation patterns of the bent antenna in Fig. 9 depicted at H-plane display similar results for all corresponding frequencies except for the bent antenna at radius of 150 mm. The radiation patterns display omnidirectional behavior with observation of more suppression at 0° and 180° of the H-plane as the frequency increases. The outlier results are contributed by the bending at 150 mm radius, depicting initial suppression at 0° and 180° and spreading further suppression at 90° and 270° with increasing frequency.

Circuit modeling of antenna bending effect: The shifts in the resonant frequencies and radiation patterns when bending the UWB antenna are mainly caused by the discontinuity in the antenna geometry, as explained in Kornek *et al*. (2010). During the bending, parts of the patch antenna are being stretched that it leads to a distortion of electrical field between the patch antenna and the ground plane. A circuit model has been derived to analyze the bending effect of the UWB antenna. Using AWR Design Environment, a lumped element

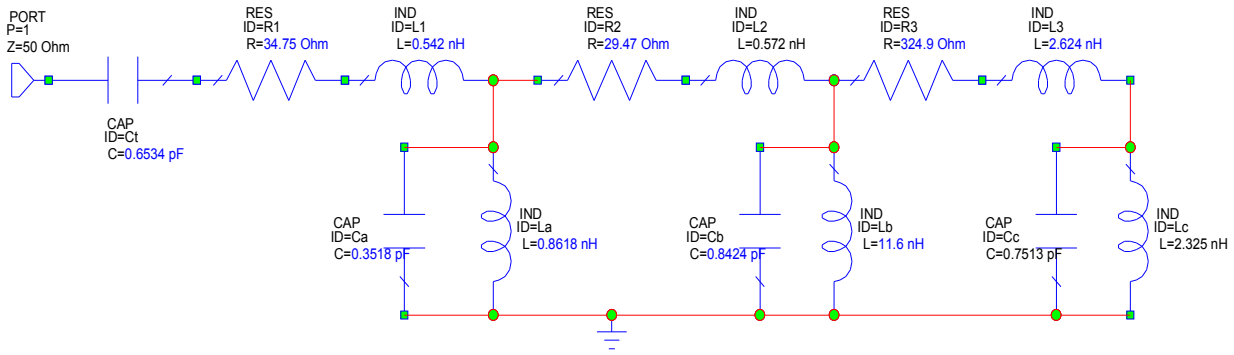

Fig. 10: Circuit modeling of UWB microstrip patch antenna

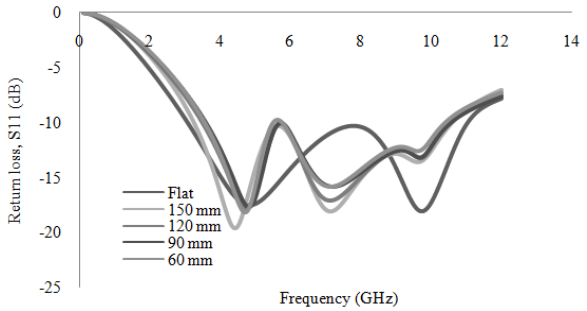

Fig. 11: Bending effect on impedance bandwidth using AWR design environment

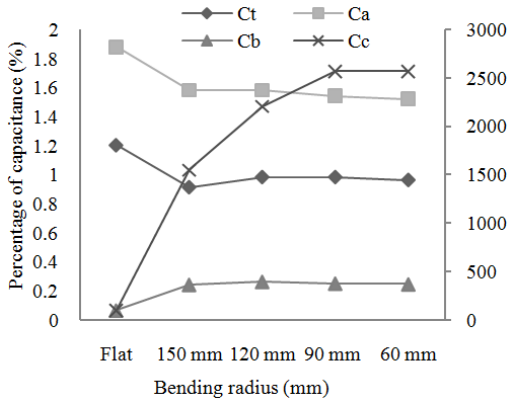

Fig. 12: Relationship between percentage of capacitance and bending radius

circuit model is first derived to replicate the performance of the UWB planar antenna, without the bending effect, as illustrated in Fig. 10. The circuit comprises three cascaded resonant circuit made up of a combination of resistor in series with inductors and capacitor in parallel. A tuning capacitor is inserted to represent the coupling between the patch and the ground. The circuit is designed and optimized so that it produces the same graph of impedance bandwidth as produced in CST Microwave Studio. Based on the analysis done, the first stage of resonant circuit is contributed by the patch length of the UWB antenna, which contributes to the first resonant frequency as seen in Fig. 2. The second resonant frequency is represented by the second stage of the circuit model, contributed by the truncated step of the patch antenna. Meanwhile, the last cascaded stage represents the notched partial ground plane of the antenna, as the notch of the ground helps in lowering the graph peak so that the return loss, S_{11} stays below -10 dB.

The circuit model is tuned and optimized to produce the results of antenna bending over all radii which are earlier obtained from CST Microwave Studio. The results are imposed on the same graph as illustrated in Fig. 11. During the bending of antenna, the discontinuity of the antenna geometry has altered the electrical field of the antenna, therefore giving a rise in the change of capacitance between the antenna elements. The relationship between the capacitance and the bending of antenna is illustrated in Fig. 12, with C_a, C_b and C_c denoting the capacitor of stage one, two and three, respectively. The tuning capacitor, C_t decreases in value which indicates that the electrical field between the patch antenna and the ground is disturbed and decreased, similar to the study done by Kornek *et al.* (2010) on antenna with MID substrate. Further bending does not affect much on the tuning capacitor as compared to the other capacitors in the circuit. As expected, the capacitive loading at the patch antenna represented by the capacitor of the first stage does decrease steadily with increasing bending angle. The magnetic field represented by the inductors does not display noticeable change. Interestingly, the deformation of the antenna shape during bending affects mostly on the components in stage two and three of the circuit model. The capacitive loading at the truncated step of the patch antenna increases drastically as soon as the antenna is bent, while depicting a steady increase with increasing bending angle. This also indicates that the electrical field is stronger at the truncated step of patch antenna which is near the ground plane. The same pattern is observed for the capacitance at stage three which is mainly responsible for the notched ground plane. The inductance also increases drastically during the antenna bending. It is known that the notch at the ground plane functions to compensate the excess capacitance to produce better matching for the antenna performance. The

discontinuity of both the truncated step of patch antenna and the ground plane due to bending effect has stretched the antenna geometry to the extent that it increases the capacitance and inductance drastically compared to other parts of the antenna. The variation of impedance matching during the antenna bending has introduced an additional resonant frequency at the return loss, S_{11} graph as seen in Fig. 6.

CONCLUSION

This study presents the effect of UWB microstrip patch antenna bending on the antenna performance, mainly on the impedance bandwidth, return loss S_{11} and radiation patterns. The effect on antenna bending causes a shift in resonant frequencies while affecting the impedance bandwidth minimally. The variation in impedance matching also introduces an additional resonant frequency during the bending. More shifts of the resonant frequencies are observed with increasing bending angle. The radiation patterns on both E-plane and H-plane display similar but broadened pattern compared to the UWB planar antenna. More analysis is conducted by developing the circuit model to replicate the UWB antenna design, of which it is observed that there is variation in terms of its capacitive and inductive loading at different parts of the antenna element. In a nutshell, UWB antenna proposed in this study is still suitable to be bent for non-planar surface application as it complies to UWB bandwidth with slight degradation yet preserving UWB characteristics.

REFERENCES

Amaro, N., C. Mendes and P. Pinho, 2011. Bending effects on a textile microstrip antenna. Proceeding of the IEEE International Symposium on Antennas and Propagation (APSURSI). Spokane, WA, July 3-8, pp: 282-285.

Bai, Q. and R. Langley, 2009. Wearable EBG antenna bending and crumpling. Proceeding of the Loughborough Antennas and Propagation Conference (LAPC). Loughborough, November 16-17, pp: 201-204.

Bai, Q. and R. Langley, 2010. Bending of a small coplanar textile antenna. Proceeding of the Loughborough Antennas and Propagation Conference (LAPC). Loughborough, November 8-9, pp: 329-332.

FCC (Federal Communications Commission), 2002. First report and order in the matter of revision of part 15 of the commission's rules regarding ultra wideband transmission systems. FCC 02-48, ET-Docket, pp: 98-153.

Galehdar, A. and D.V. Thiel, 2007. Flexible, light-weight antenna at 2.4GHz for athlete clothing. Proceeding of the IEEE Antennas and Propagation Society International Symposium. Honolulu, HI, June 9-15, pp: 4160-4163.

Hoefer, W.J.R., 1977. Equivalent series inductivity of a narrow transverse slit in microstrip. IEEE T. Microw. Theory, 25(10): 822-824.

Kellomaki, T., J. Heikkinen and M. Kivikoski, 2006. Effects of bending GPS antennas. Proceeding of the Asia-Pacific Microwave Conference (APMC). Yokohama, December 12-15, pp: 1597-1600.

Kornek, D., E. Slottke, C. Orlob and I. Rolfes, 2010. Experimental investigation of bent patch antennas on MID substrate. Proceedings of the 4th European Conference on Antennas and Propagation (EuCAP). Barcelona, Spain, April12-16, pp: 1-3.

Salonen, P. and Y. Rahmat-Samii, 2007. Textile antennas: Effects of antenna bending on input matching and impedance bandwidth. IEEE Aero. El. Sys. Mag., 22(3): 10-14.